Bioaccumulation of per- and polyfluoroalkyl substance in fish from an urban river: occurrence, patterns and investigation of potential ecological drivers

Nicolas Macorps[1], *Karyn Le Menach*[1], *Patrick Pardon*[1], *Sabrina Guérin-Rechdaoui*[2], *Vincent Rocher*[2], *Hélène Budzinski*[1], *Pierre Labadie*[1*]

[1] CNRS/Université de Bordeaux, UMR 5805 EPOC, Talence, France

[2] SIAAP, Direction Innovation, Colombes, France

*Corresponding author.

E-mail address: pierre.labadie@u-bordeaux.fr

Published in Environmental Pollution, accepted in March 2022

https://doi.org/10.1016/j.envpol.2022.119165

Abstract

Per- and polyfluoroalkyl substances (PFAS) are ubiquitous in aquatic environments and a recent shift toward emerging PFAS is calling for new data on their occurrence and fate. In particular, understanding the determinants of their bioaccumulation is fundamental for risk assessment purposes. However, very few studies have addressed the combined influence of potential ecological drivers of PFAS bioaccumulation in fish such as age, sex or trophic ecology. Thus, this work aimed to fill these knowledge gaps by performing a field study in the Seine River basin (France). Composite sediment and fish (European chub, *Squalius Cephalus*) samples were collected from four sites along a longitudinal transect to investigate the occurrence of 36 PFAS. Sediment molecular patterns were dominated by fluorotelomer sulfonamidoalkyl betaines (i.e. 6:2 and 8:2 FTAB, 46% of ∑PFAS on average), highlighting the non-negligible contribution of PFAS of emerging concern. C_9–C_{14} perfluoroalkyl carboxylic acids, perfluorooctane sulfonic acid (PFOS), perfluorooctane sulfonamide (FOSA) and 10:2 fluorotelomer sulfonate (10:2 FTSA) were detected in all fish samples. Conversely, 8:2 FTAB was detected in a few fish from the furthest downstream station only, suggesting the low bioaccessibility or the biotransformation of FTABs. ∑PFAS in fish was in the range 0.22–3.8 ng g^{-1} wet weight (ww) and 11–140 ng g^{-1} ww for muscle and liver, respectively. Fish collected upstream of Paris were significantly less contaminated than those collected downstream, pointing to urban and industrial inputs. The influence of trophic ecology and biometry on the interindividual variability of PFAS burden in fish was examined through analyses of covariance (ANCOVAs), with sampling site considered as a categorical variable. While the latter was highly significant, diet was also influential; carbon sources and trophic level (i.e. estimated using C and N stable isotope ratios, respectively) equally explained the variability of PFAS levels in fish.

Keywords

PFAS; emerging contaminants; fish; sediment; bioaccumulation

Highlights

- Emerging PFAS (*e.g.* zwitterionic compounds) largely contributed to the molecular pattern observed in sediments
- PFAS levels along the river transect were influenced by urban/industrial inputs
- Along with legacy PFAS, the fluorotelomer sulfonate 10:2 FTSA was ubiquitous in chub
- PFAS bioaccumulation was controlled by site contamination and fish diet

1. Introduction

Per- and polyfluoroalkyl substances (PFAS) are a group of persistent molecules that have been extensively monitored in the environment and human populations for over 20 years (Giesy and Kannan, 2001; Hansen et al., 2001). Perfluoroalkyl carboxylates (PFCAs) and perfluoroalkyl sulfonates (PFSAs) have been reported to be widely distributed in aquatic ecosystems, including biota (Ahrens, 2011). Perfluorooctane sulfonate (PFOS) and its salts, as well as perfluorooctane carboxylate (PFOA), have been listed under Annexes B and A of the Stockholm Convention, respectively. This pushed towards the production of replacements of long-chain PFAS like perfluoroether sulfonic acid (PFESAs) and carboxylic acid (PFECAs) (Xiao, 2017).

As a consequence, emerging PFAS were detected in surface water and sediments in recent years (De Silva et al., 2011; Pan et al., 2018; Joerss et al., 2019; Chen et al., 2020). These include PFESAs and PFECAs like F-53B, a chlorinated PFESA mainly used in the electroplating industry in China as PFOS alternative (Wang et al., 2013), HFPO-DA (trade name GenX), ADONA, used as replacement for PFOA as processing aid in fluoropolymer manufacturing (Munoz et al., 2019) or perfluoroethylcyclohexane sulfonate (PFECHS), found in hydraulic fluids but phased out since 2002 (De Silva et al., 2011). PFECHS presents a lower bioaccumulation factor (BAF) than PFOS in *Carassius carassius* (Wang et al., 2016) while the contrary is observed for 6:2 Cl-PFESA in zebrafish (Tu et al., 2019). The latter was reported in Greenland marine mammals (Gebbink et al., 2016), fish and marine organisms from China (Shi et al., 2015; Liu et al., 2017; Wang et al., 2021). HFPO-DA and ADONA have never been measured in aquatic biota and exhibit low bioaccumulation potential (Munoz et al., 2019). Other alternatives that may be transformed into perfluoroalkyl acids (PFAAs) are also of concern (Zabaleta et al., 2017), like fluorotelomer betaines (FTABs), used in aqueous film forming foam formulations (AFFFs) (Place and Field, 2012), and fluorotelomer

sulfonates (FTSAs), used as a PFOS replacement (Field and Seow, 2017). FTABs were previously detected in river sediments at selected locations in France (Munoz et al., 2016). 8:2 FTAB was also found in sediment and fish from Lake Mégantic and Chaudière River (Canada) after a railway accident, with a gradual concentration decrease within a few years (Munoz et al., 2017b). Furthermore, 8:2 FTSA and 10:2 FTSA were also detected in the Chaudière River after this accident and the latter was also ubiquitous in biota from a small urban river in France (Simonnet-Laprade et al., 2019). Thus, the ever increasing number of identified and detected PFAS advocate for further studies, especially in urban rivers, based on extended lists of target compounds (Simonnet-Laprade et al., 2019).

In addition, the controlling factors of PFAS bioaccumulation in fish are still not fully understood, although some drivers have been identified. PFAS bioaccumulation can be affected by their structural characteristics such as chain length (i.e. competition between short and long-chain PFAS) and functional group (Labadie and Chevreuil, 2011; Wen et al., 2017; Lee et al., 2020). In addition, the absorption, distribution, metabolism, and elimination of these chemicals is controlled by complex interaction with biomolecules such as proteins, transporters, and phospholipids (de Silva et al., 2021). However, other environmental factors might also be at play. At some locations, the burden of long-chain PFAS was correlated with fish length (*i.e.* proxy for age, Mann, 1976) (Lam et al., 2014; Babut et al., 2017), while no association was observed at other sites (Åkerblom et al., 2017; Langberg et al., 2019). At some Nordic locations, ∑PFAS was negatively correlated with δ^{15}N (*i.e.* proxy for trophic position), suggesting the absence of biomagnification (Lescord et al., 2015; Åkerblom et al., 2017), while trophic magnification factors > 1 were reported elsewhere (Loi et al., 2011; Simonnet-Laprade et al., 2019). Using δ^{15}N and δ^{13}C (i.e. proxy for carbon sources) as indicators of trophic ecology, diet was identified as a relevant factor to explain the interspecific bioaccumulation pattern of long-chain PFAS in fish from the Rhone River, e.g.

perfluorononanoic acid (PFNA), perfluoroundecanoic acid (PFUnDA), PFOS and perfluorooctane sulfonamide (FOSA) (Babut et al., 2017). Overall, studies combining a wide array of proxies to explain the interindividual (i.e. intraspecific) variability of PFAS contamination levels are relatively scarce. Understanding the relative influence of bioaccumulation determinants is, however, of primary importance for predicting PFAS burden and for risk assessment purposes (Lopes et al., 2011).The drivers of the intraspecific variability of PFAS burden have generally been studied independently; they are still poorly documented and clearly deserve deeper investigation. This is a major issue to get further insight into the dynamics of PFAS in trophic webs but also to implement biota monitoring strategies, e.g. in the context of the European Water Framework Directive (Fliedner et al., 2018).

In this context, the present study focused on the heavily urbanized Seine River basin and on an omnivorous cyprinid, the European Chub *Squalius Cephalus*, frequently used in biomonitoring studies as it is widely distributed in European freshwaters (Labadie and Chevreuil, 2011; (Nyeste et al., 2019). Previous studies have demonstrated the widespread occurrence of PFAS in this river (Labadie and Chevreuil, 2011; Munoz et al., 2018), resulting from diffuse and point sources (i.e. fluorochemical plant and waste water treatment plants). To investigate the potential contamination gradient induced by urban and industrial inputs into the Seine River, an extended list of legacy and infrequently reported emerging compounds was analyzed. We explored the PFAS spatial variability in sediment and fish along a longitudinal transect, i.e. upstream and downstream of the Greater Paris conurbation. Furthermore, tissue distribution was considered (i.e. dorsal muscle vs liver) and we aimed to investigate the potential ecological drivers of PFAS bioaccumulation and its intraspecific variability in a model fish species, through multivariate analysis (i.e. considering biometry and indicators of trophic ecology).

2. Material and Methods

2.1. Chemicals.

The full list of reagents and chemicals is provided in the Supporting information (SI). Certified native PFAS (i.e. not mass-labeled) (n = 36, chemical purity >98%) and isotope-labeled internal standards (ISs) (n = 20) (isotopic purity >94%) were acquired from Wellington Laboratories (BCP Instruments, Irigny, France), except 8:2 FTAB that was synthesized by Innovorga (Reims, France) (> 98 %). Native PFAS included PFCAs (C_5–C_{14}), PFSAs (C_4, C_6–C_8, C_{10}), one polyfluoroalkyl carboxylate (5:3 FTCA, also termed FPePA), FTSAs (4:2 FTSA, 6:2 FTSA, 8:2 FTSA and 10:2 FTSA), FOSA and its *N*-alkylated derivative (N-MeFOSA), perfluorooctane sulfonamide acetic acids (FOSAA, N-MeFOSAA, N-EtFOSAA), FTABs (6:2 FTAB and 8:2 FTAB), fluorotelomer phosphate diesters (6:2 diPAP and 8:2 diPAP), chlorinated PFESA (6:2 Cl-PFESA and 8:2 Cl-PFESA, i.e. major and minor components of F-53B, respectively) and fluoroalkyl ethers (HFPO-DA and ADONA). L-PFOS herein refers to the linear isomer of PFOS and Br-PFOS to the sum of branched isomers. Analyte name, acronym and corresponding internal standard (IS) are provided in Table S1.

2.2. Study site

The Seine River flows through the Greater Paris with a relatively low mean daily discharge of 312 $m^3.s^{-1}$ over the 1974–2021 period. This flow is lower in summer, i.e. 150 $m^3.s^{-1}$ on average over the last 20 years, especially in 2019 (< 100 $m^3.s^{-1}$) (BanqueHydro). The Seine River basin is under a strong urban influence, hosting a population of approximately 16 million inhabitants.

Based on the hypothesis of a longitudinal contamination gradient in the Seine River basin due to urban inputs, the sampling strategy relied on the fish monitoring scheme implemented for over two decades on the Seine and Marne rivers by the SIAAP MeSeine network (Azimi and Rocher, 2016). Four sampling sites were investigated (Figure S1). Gournay-sur-Marne (48.51° N, 2.34° E), located on the Marne River 25 km upstream from its confluence with the Seine River, was used as a relative reference site not directly impacted by the Paris conurbation (Goutte et al., 2018). Levallois (48.54° N, 2.17° E) and Le Pecq (48.53° N, 2.06° E), are situated on the Seine River, 10–30 km downstream of Paris. The farthest downstream site, Triel-sur-Seine (48.98° N, 2.00° E), is located downstream of the Seine and Oise river confluence; it was selected to integrate inputs from the Paris conurbation as well as those from a fluorochemical plant located in the Oise River watershed (Boiteux et al., 2017).

2.3. Sampling

Composite surface sediment samples (0–2 cm, n = 1 per site) were collected in August 2019 at each location with a stainless-steel spoon and kept in aluminum containers at 4°C. Upon arrival at the laboratory, samples were stored at -20°C until further analysis.

European Chub samples were collected at the same time than sediments, according to Azimi and Rocher (2016). This bentho-pelagic species is frequently used for biomonitoring studies as chubs are very abundant in European rivers (Caffrey et al., 2008). In addition, *S. cephalus* are long-lived omnivorous fishes with large interindividual diet variations (Balestrieri et al., 2006). Fish were collected by electrofishing (n = 10–12 per site), anesthetized (MS222, 1 $g.L^{-1}$ in river water) and euthanized. After sacrifice, sex was determined based on gonad morphology for each individual, then length and weight were recorded (Table S6). Individuals were dissected on site to collect liver (n = 45) and fillets (dorsal muscle) (n = 46). Tissues

were stored in polypropylene tubes in a cooler (4°C) and then stored at -20°C upon arrival at the laboratory and until further analysis.

2.4. PFAS analysis

Sediment samples were freeze-dried, sieved at 2mm, ground with a ball mill and homogenized before analysis. Fish tissues were also freeze-dried, ground and homogenized. Fish samples were prepared using a procedure adapted from a previous study by our group (Simonnet-Laprade et al., 2019). Briefly, prior to microwave-assisted solvent extraction using 12 mL of MeOH + 100 mM NaOH (10 min, 70°C), ISs (2 ng each) were added to fish tissues (muscle: 200 mg dry weight (dw); liver: 50 mg dw). Extracts were sequentially cleaned-up on Strata X-AW and ENVI-Carb cartridges before concentration to 300 µL (N_2, 45°C), transfer to polypropylene injection vials and storage at -20°C until analysis. Sediment samples (1g dw) were processed similarly but clean-up was performed on ENVI-Carb cartridges only. PFAS analyses were performed using liquid chromatography coupled with tandem mass spectrometry on a 1290 LC system interfaced with a 6495 triple quadrupole mass spectrometer from Agilent Technologies (Massy, France). Further details on chromatographic conditions and mass spectrometry parameters are provided in the SI (Table S2).

Procedural blank consisted of extraction solvent supplemented with ISs. For analytes quantified in procedural blanks (Table S3), data were blank-corrected. Limits of detection (LoDs), based on either blanks or signal-to-noise ratios as described elsewhere (Munoz et al., 2015), were in the range 0.005–1.0 ng g^{-1} wet weight (ww), 0.02–1.0 ng g^{-1} ww and 0.05–0.45 ng g^{-1} dw for fish muscle, liver and sediment respectively (Table S4). The limits of quantification (LoQs) were determined as 10/3*LoD.

2.5. Quality assurance and quality control

Whole method recovery rates were assessed through the analysis of common sole (*Solea solea*) fillets from the Gironde estuary (n = 9, fortified at 5 ng.g^{-1} ww) and sediment from the Orge River (n = 3, fortified at 5 ng g^{-1} dw); recoveries ranged between 50 and 105% for all but two analytes in fish muscle, while they were in the range 48–91% for sediments, except for FTABs (Table S5). Accuracy was determined with common sole fillets (n = 16) and sediment (n = 3) spiked with ISs and analytes at the beginning of the procedure (5 ng g^{-1} each). It was in the range 80–120% in spiked sediment and 52–119% in fish tissues, with relative standard deviation (RSD) between 6 and 21%, except for 6:2 FTAB and 8:2 FTAB (Table S5). The overall lower performances for the determination of FTABs in a complex matrices are not unexpected, considering the lack of appropriate ISs (i.e. isotopologues) and the structural differences with anionic PFAS. This led to the overestimation of their concentration in fish tissues (factor 1.4–1.7) and to the underestimation of their concentrations in sediments (factor 2.9–3.3), which did not affect our conclusions (e.g. see molecular patterns in section 3.2).

2.6. Stable isotope analysis

The isotopic composition of fish fillets was evaluated on defatted tissues (Bodin et al., 2009; Simonnet-Laprade et al., 2019). Samples (0.2 ± 0.1 mg) were weighed in tin capsules and stable isotope ratios were determined using a ThermoFinnigan Delta V elemental analyzer (EA-IRMS) with a Conflo IV interface. Carbon and nitrogen isotopic compositions were expressed as per mil (‰) in the δ notation relative to Vienna Pee Dee Belemnite (VPDB) and atmospheric N_2, respectively. Trueness was assessed through replicate analyses (every 10–12 samples) of IAEA-N2 (δ^{15}N = 20.3‰) and USG-24 (δ^{13}C = -16.05 ± 0.1‰) reference

materials and averaged 20.25 ± 0.23 (n = 10) and -15.94 ± 0.35 (n = 18) for δ^{15}N and δ^{13}C respectively.

2.7. Statistics

The R statistical software (R version version 4.0.5 R core team 2021) was used to perform statistical analyses. Values <LoD were replaced by 0.5 × LoD and PFAS with detection frequency (DF) < 50 % were not considered for statistics. Since data were not normally distributed (Shapiro-Wilk W-test), statistical differences between groups were perform with Mann-Whitney (paired comparison) or Kruskall-Wallis (comparison of several samples) test, followed by Dunn post-hoc procedure with Bonferroni correction for multiple comparison to specify which groups differed from the others. The Spearman's rank correlation coefficient was used to investigate correlation between individual PFAS and between liver and muscle PFAS concentrations. Analysis of covariance (ANCOVA) was performed to explore the influence of potential explanatory variables (*i.e.* length, weight, δ^{15}N and δ^{13}C) on contamination levels; sampling site was considered as a qualitative variable. Variables were centered and reduced to estimate their relative contribution to the regression models. For each model, significant variables were determined by type III sum of square analysis and the improvement of models resulting from the removal of non-significant variables was assessed by the partial F-test. For all analyses, the significance threshold was set at 0.05.

3. Results And Discussion

3.1. Fish biometry and trophic ecology.

To acquire a robust dataset, 46 individuals were collected (i.e. 10–12 *per* sampling site). Fish length ranged from 176 to 500 mm and from 170 to 354 mm for females and males respectively; weight ranged from 56 to 1572 g and from 47 to 419 g for females and males, respectively. Thus, individuals displayed contrasting features (Table S6) with a RSD of 28% and 103% for length (proxy for fish age) and weight, respectively. No significant difference in length or weight distribution was observed between sampling sites. Based on results acquired in the same biogeographical area and using length as proxy for age, most sampled individuals were likely sexually immature (Mann, 1976).

$\delta^{13}C$ and $\delta^{15}N$ values ranged from -24.26 to -27.82 ‰ (mean -26.70 ± 0.74 ‰) and 9.40 to 13.32 ‰ (mean 11.47 ± 0.90 ‰), respectively (Figure 1). The wide range of $\delta^{13}C$ values are in good agreement with the variety of carbon sources utilized by this omnivorous species (Marković et al., 2007). Nitrogen isotope ratios were significantly different between sites, with higher $\delta^{15}N$ values at Triel-sur-Seine than at Le Pecq and Gournay-sur-Marne. This $\delta^{15}N$ enrichment may be linked to inputs from a large wastewater treatment (WWTP) (Hicks et al., 2017; Munoz et al., 2018) located a few km upstream (Hicks et al., 2017; Munoz et al., 2018). The lower variability of isotopic ratios at Triel-sur-Seine may also indicate a specialization in *S. cephalus* diet (Hette Tronquart et al., 2016). Overall, inter-individual differences are likely due to sampling site specificities and to the omnivorous diet of *S. cephalus*.

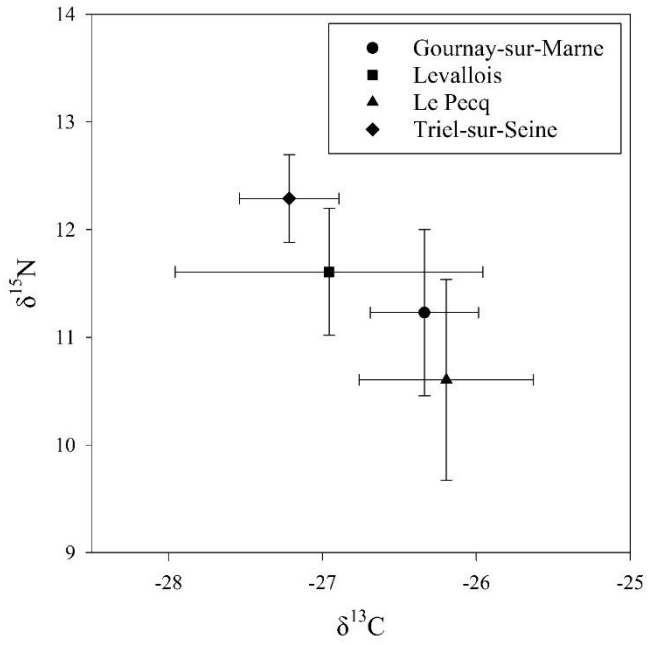

Figure 1. Mean stable isotope signature (δ^{15}N vs δ^{13}C) in European chub fillets collected in the Seine River basin (error bars represent standard deviations)

3.2. PFAS concentrations and patterns in sediments

Analysis of surface sediments provided a time-integrated estimation of PFAS contamination at the different sampling sites. Among the 36 analyzed PFAS, 17 were detected in this compartment (Table S7). L-PFOS, Br-PFOS, PFDoDA and 6:2 FTAB were systematically detected; 5:3 FTCA was detected at all sites except Le Pecq and 8:2 FTAB levels were > LOD at two sites (Levallois and Triel-sur-Seine). PFAA alternatives such as 6:2 and 8:2 Cl-PFESA or HFPO-DA were never detected but ADONA was quantified at two sites, albeit at low levels (< 0.04 ng.g^{-1} dw). The low detection frequency of these compounds compared to a recent report for the Bohai Bay, China (Chen et al., 2020), illustrates the weakness of their current emissions in the Seine River basin (i.e. few or no industrial sources). ∑PFAS was in the range 0.78–6.7 ng g^{-1} dw, with individual compounds generally below ng g^{-1} level (Table

S7) except 6:2 FTAB at Triel-sur-Seine (1.70 ± 0.07 ng g^{-1} dw). Concentrations were in the same order of magnitude than those previously observed in the Seine River (Munoz et al., 2018) and in the nearby Orge River (mean ∑PFAS = 2.28 ± 2.31 ng g^{-1} dw) (Simonnet-Laprade et al., 2019). At all sites, molecular patterns were dominated by 6:2 FTAB that accounted for 46 ± 19% of ∑PFAS, followed by 5:3 FTCA and L-PFOS (18 ± 14% and 14 ± 4%, respectively); this clearly provided evidence for the non-negligible contribution of several PFAS of emerging concern (Figure S2). A peculiar PFAS pattern was observed at Triel-sur-Seine, i.e. the presence of 6:2 FTSA (2.6 ± 0.8% of ∑PFAS). Additionally, when PFAS levels were normalized to the total organic carbon content, sediments collected at Triel-sur-Seine appeared more contaminated than those from the further upstream locations. Conversely, Munoz et al. (2018) found no contamination gradient on this river stretch. The difference with our study may arise from specific hydrological conditions, i.e. the particularly low flow rate of the Seine River observed during summer 2019 may have reduced the dilution capacity and sediment transport at the most downstream site. The extended list of PFAS targeted herein (e.g. inclusion of FTABs) may also explain this discrepancy. For instance, 6:2 FTAB proved to be ubiquitous in French river sediments (Munoz et al., 2016) and predominant in sediments from the Oise River collected downstream of a fluorochemical manufacturing plant (Boiteux et al., 2017), thus likely contributing to the higher levels of this compound at Triel-sur-Seine. Inputs from this plant also possibly make for the increased 6:2 FTSA contribution, as observed in periphytic biofilm from the same site (Munoz et al., 2018). The presence of FTSAs in the Seine River could directly originate either from the use or production of these compounds or from the biotransformation of precursors such as fluorotelomer sulfonamidoalkyl betaines found in AFFF formulations (Field and Seow, 2017). The peculiar molecular pattern observed at the most downstream site may also be attributed to increased WWTP inputs (Munoz et al., 2018).

3.3. PFAS levels and patterns in fish

Across all sampling sites, C_{10}–C_{14} PFCAs, L-PFOS, FOSA and 10:2 FTSA were detected in all fish (Table 1). MeFOSAA was also frequently detected in muscle (96%) while PFOA and PFDS were routinely detected in liver (91% and 98%, respectively). Conversely, most emerging PFAS were less frequently reported. For instance, 8:2 FTSA was more rarely detected than 10:2 FTSA (22 % and 58 % of muscle and liver samples, respectively), while PFECHS was found in 20% of liver samples only and 8:2 Cl-PFESA was detected in a single liver sample at Le Pecq. This further suggests that these PFAS are not widely emitted in the Seine River basin yet. Although FTABs were present in sediments, 6:2 FTAB was never detected in fish and 8:2 FTAB was detected in only 4 individuals from Triel-Sur-Seine, at low level (<LoQ).

∑PFAS was in the range 0.22–3.8 ng g^{-1} ww and 11–140 ng g^{-1} ww in muscle and liver, respectively (Table 1); this resulted in an interindividual variability of 52% and 47%, respectively. ∑PFAS was in the same order of magnitude than those reported for *S. cephalus* elsewhere in Europe. Such concentrations were actually in the same range than those reported for other freshwater ecosystems in France (Babut et al., 2017; Simonnet-Laprade et al., 2019) or Germany (Fliedner et al., 208), but somewhat lower than those observed in the Czech Republic (Cerveny et al., 2016) (i.e. up to 38 ng g^{-1} ww in fillets). Higher levels in liver than in muscle are consistent with PFAS affinity for specific proteins, e.g. liver fatty acid-binding proteins (Labadie and Chevreuil, 2011).

As regards individual PFAS, the highest concentrations were observed for L-PFOS (0.63–13 ng g^{-1} ww and 5.8–94 ng g^{-1} ww in muscle and liver, respectively) and even-number long-chain PFCAs: PFDoDA (0.37–5.0 ng g^{-1} ww and 1.6–18 ng g^{-1} ww in muscle and liver, respectively) and PFTeDA (0.22–3.8 ng g^{-1} ww and 0.66–12 ng g^{-1} ww in muscle and liver, respectively). These results were expected due to the greater bioaccumulation potential of long-chain PFAS (Labadie and Chevreuil, 2011). PFOS is regulated under the European Water Framework directive and an environmental quality standard for biota (EQS_{biota}) was set up to protect "Human health via consumption of fishery products", i.e. 9.1 ng g^{-1} ww (European Commission, 2013). For chub, whole-body PFOS concentrations can be estimated based on concentrations in fillets and using a conversion factor of 1.908 (Simmonet-Laprade et al., 2019). The exceedance frequency was quite low (i.e. 6.5 % of analyzed fish) but EQS_{biota} compliance for PFOS was observed at two sites only, since levels in two individuals from Levallois and a single one from Le Pecq exceeded the threshold value of 9.1 ng g^{-1} ww. This provides further evidence that despite PFOS phase-out in Europe, the contamination of hydrosystems by this chemical remains a long-term environmental issue. The median concentrations of other long-chain PFCAs were in the range <0.03–1.6 ng g^{-1} ww and 0.12–10 ng g^{-1} ww in muscle and liver, respectively (Figure 2). The bioaccumulation of the fluorotelomer 10:2 FTSA has seldom been reported so far. Here, its median concentrations were 0.13 ng g^{-1} ww and 0.74 ng g^{-1} ww in muscle and liver, respectively. Noteworthy, such values are lower than those observed for PFCAs but much larger than those reported herein for other PFAA precursors. The concentration range of this often overlooked compound was similar to that reported for other cyprinids from the nearby Orge River (Simonnet-Laprade et al., 2019) but lower than those observed in the Chaudiere River following the massive use of AFFFs (Munoz et al., 2017b).

In fish tissues, ∑PFAS and several individual compounds exhibited significant spatial differences (Table S9). Fish from Gournay-sur-Marne displayed lower levels of ∑PFAS, ∑PFOS, 10:2 FTSA and FOSA compared to those observed at all downstream sites on the Seine River. Although, the highest median ∑PFAS was measured at Levallois, PFAS levels in fish did not differ between sites located downstream of Paris. A contamination gradient in the Seine River was previously observed for dissolved PFAS (Munoz et al., 2018) and for other micropollutants in sediment and fish (Teil et al., 2014). Here, we found lower PFAS levels upstream of Paris, which further confirms the impact of dense urban areas on the Seine River contamination. Note that we did not investigate a strict longitudinal gradient since the upstream site was located on the Marne River; however, similar trends were reported for trace metals and Gournay-Sur-Marne can be considered as a suitable reference site at regional scale (Elbaz-Poulichet et al., 2006; Grosbois et al., 2006).

As stated above, L-PFOS and long-chain carboxylates were the dominant compounds in chub; this is consistent with previous findings in freshwater fish (Labadie and Chevreuil, 2011; Ahrens et al., 2015; Simonnet-Laprade et al., 2019). The relative abundance of emerging PFAS was also examined. When detected, the contribution of 5:3 FTCA to ∑PFAS in muscle was in the range 5–9 % (n = 3) while PFECHS contribution in liver was in the range 0.5–1.8%.

The contribution of FTSAs significantly increased at Triel-Sur-Seine. For instance, 10:2 FTSA accounted at this site for 2.3 ± 0.5% and 1.9 ± 0.4% of ∑PFAS in muscle and liver, respectively. At this site, 6:2 FTSA was found in liver and 8:2 FTSA in both liver and muscle, but their contribution to ∑PFAS was low (i.e. < 1 %) partly because of their lower bioaccumulation potential. This specific pattern is likely related to industrial inputs (Munoz et al., 2015). When detected, 8:2 FTAB contribution was similar to that of 10:2 FTSA in muscle. Very few data are available for FTSAs and the existing studies mostly focused on 6:2 FTSA

(Butt et al., 2014; Zhang et al., 2021). Ahrens et al. (2015) found a higher contribution of 6:2 FTSA to ∑PFAS in gonads and lower relative contribution of this compound to ∑PFAS in liver and muscle tissues of *Perca fluviatilis* near Stockholm Arlanda Airport. Our results suggest that a similar relative abundance can be expected for 10:2 FTSA in muscle and liver (Figure 2).

Correlations among individual PFAS were examined separately for muscle and liver samples (Figure S3). Positive associations were observed between most compounds in both matrices, with a few exceptions. For instance, only 10:2 FTSA and PFTeDA were not correlated with each other in liver, suggesting a different behavior between these two compounds (i.e. a PFAA precursor and a potential biotransformation end product). In muscle, PFTrDA and PFTeDA were correlated with neither 10:2 FTSA nor FOSA but showed significant associations with other PFAS. Potential sources for these compounds include the biotransformation of precursors (Ahrens, 2011).

For each sampling location, biota-to-sediment accumulation factors (BSAFs) were calculated for selected emerging PFAS and for PFOS (i.e. considered as benchmark compound) (Table S8). For the sake of comparison with the literature, BSAFs were calculated in two ways, i.e. based on PFAS concentrations in sediments expressed either on a dry weight basis (BSAF) or normalized to the total organic carbon content ($BSAF_{OC}$). Overall, log $BSAF_{OC}$ were less variable than logBSAF values (i.e. lower relative standard deviation), thereby highlighting the usefulness of OC normalization. It appeared that the log $BSAF_{OC}$ of these emerging PFAS were lower than those of L-PFOS (in the range -2.3 – -1.1 vs -1.3 – 0.01). The low log $BSAF_{OC}$ of 8:2 FTAB may result from its strong binding with sediment particles *via* electrostatic interactions with negatively charged organic matter (Barzen-Hanson et al., 2017; Munoz et al., 2017b). In addition, 6:2 FTAB exhibited a lower biota-to-soil accumulation factor than PFOS (Munoz et al., 2020). This may also be related to efficient

biotransformation, as observed in zebrafish (Shi et al., 2019). Likewise, other sulfonamide betaines also proved to be metabolized into PFAAs in earthworm (Jin et al., 2020). 5:3 FTCA may result from the aerobic or anaerobic biotransformation of fluorotelomer-based compounds (Liu et al., 2010; Chen et al., 2019). . In particular, it has been suggested as a marker of landfill leachate (Allred et al., 2015; Hamid et al., 2020). Although frequently detected in sediments, 5:3 FTCA was quantified in three fish muscle samples only, which illustrates its low bioaccumulation potential. Nevertheless, it seemingly displayed the highest log $BSAF_{OC}$ of emerging PFAS; calculations were, however, performed on a limited number of samples (n=3) and results are therefore given as indicative values. Finally, 10:2 FTSA displayed intermediate BSAF, somewhat lower those previously reported for this compound (Munoz et al., 2017b).

Table 1. PFAS occurrence in European chub muscle and liver (all sites considered) (DF: detection frequency).

	Muscle (n = 46)			Liver (n = 46)		
	DF (%)	Range ($ng.g^{-1}$ ww)	Median ($ng.g^{-1}$ ww)	DF (%)	Range ($ng.g^{-1}$ ww)	Median ($ng.g^{-1}$ ww)
PFHxA	0	<0.02	<0.02	0	<0.02	<0.02
PFHpA	2	<0.005–0.02	<0.005	0	<0.005	<0.005
PFOA	2	<0.06–0.13	<0.06	33	<0.06–0.26	<0.06
PFNA	28	<0.03–0.11	<0.03	91	<0.03–0.78	0.12
PFDA	100	0.09–1.6	0.58	100	0.56–10	2.8
PFUnDA	100	0.06–1.2	0.35	96	<0.53–5.1	1.7
PFDoDA	100	0.37–5.0	1.6	100	1.6–18	7.0
PFTrDA	100	0.07–1.6	0.39	100	0.25–3.3	1.0
PFTeDA	100	0.22–3.8	0.90	100	0.66–12	3.1
PFBS	0	<0.07	<0.07	0	<0.42	<0.42
PFHxS	11	<0.02–0.10	<0.02	42	<0.17–1.6	<0.17
PFHpS	2	<0.05–0.09	<0.05	44	<0.32–0.66	<0.32
Br-PFOS	93	<0.06–3.29	0.14	100	1.1–7.6	3.2
L-PFOS	100	0.63–13.3	2.6	100	5.8–94	28.7
PFDS	28	<0.06–0.27	<0.06	98	<0.10–1.5	0.27
4:2 FTSA	0	<0.004	<0.004	0	<0.02	<0.02
6:2 FTSA	0	<0.12	<0.12	18	<0.12–0.37	<0.12
8:2 FTSA	22	<0.01–0.03	<0.01	58	<0.02–0.42	0.08
10:2 FTSA	100	0.03–0.24	0.13	100	0.16–1.5	0.74
FOSAA	0	<0.008	<0.008	0	<0.05	<0.05
N-MeFOSAA	96	<0.05–0.09	0.07	58	<0.28–0.50	0.31
N-EtFOSAA	0	<0.15	<0.15	24	<0.002–0.02	<0.002
FOSA	100	0.01–0.14	0.05	100	0.04–0.70	0.20
N-MeFOSA	0	<0.01	<0.01	0	<0.06	<0.06
6:2 diPAP	4	<1.0–2.1	<1.0	7	<1.0–4.0	<1.0
8:2 diPAP	9	<0.08–0.27	<0.08	2	<0.21–1.2	<0.21
6:2 FTAB	0	<0.34	<0.34	0	<2.0	<2.0
8:2 FTAB	9	<0.13–0.20	<0.13	2	<0.47–0.77	<0.47
HFPO-DA	0	<0.30	<0.30	0	<0.35	
ADONA	0	<0.01	<0.01	0	<0.01	<0.01
6:2 Cl-PFESA	0	<0.01	<0.01	0	<0.06	<0.06
8:2 Cl-PFESA	0	<0.006	<0.006	2	<0.20–0.22	<0.20
PFECHS	0	<0.19	<0.19	20	<0.46–0.66	<0.46
5:3 FTCA	7	<0.09–0.75	<0.09	0	<0.36	<0.36
∑PFAS	**100**	**0.22–3.8**	**7.4**	**100**	**11–140**	**54**

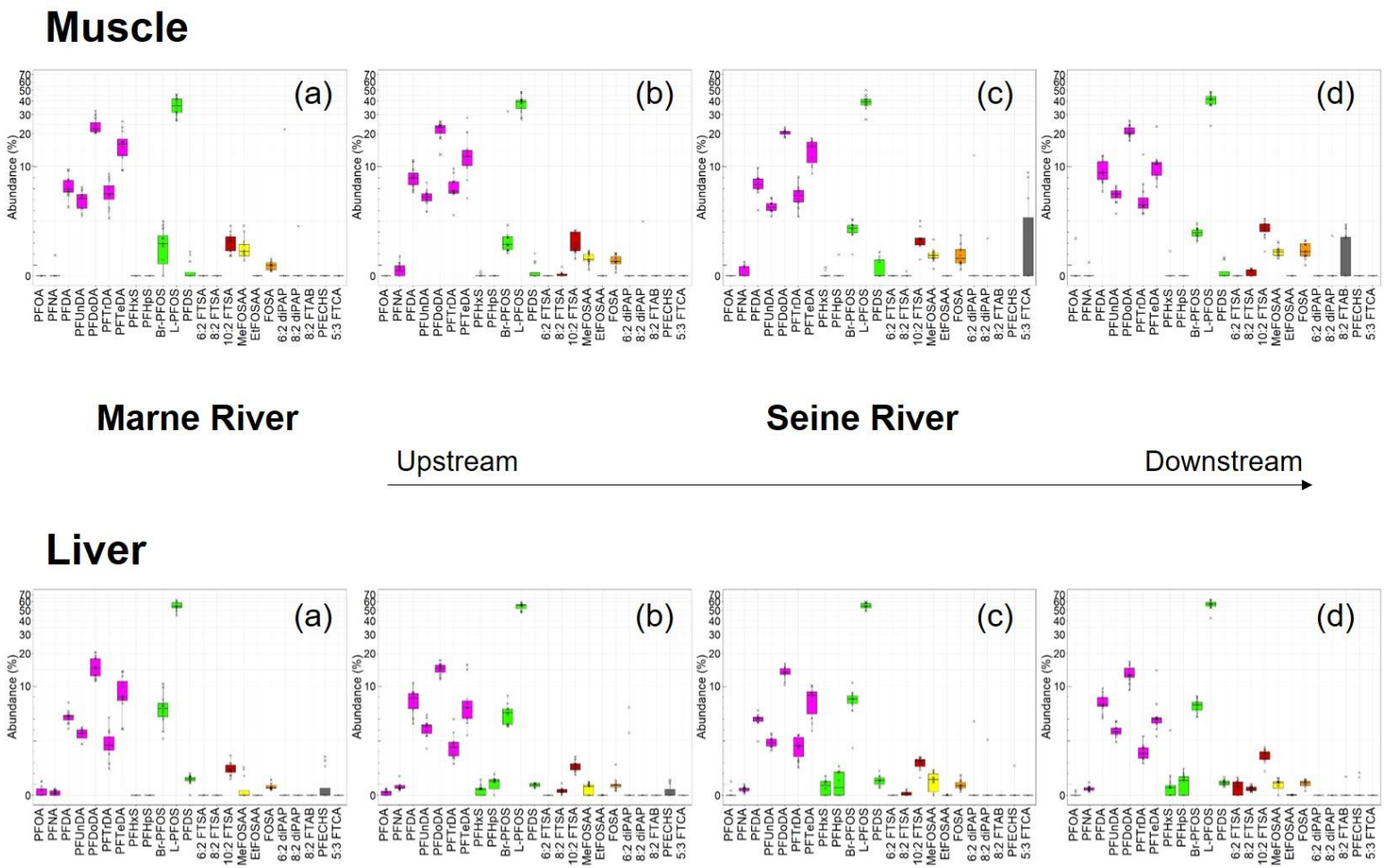

Figure 2. Relative contribution of individual PFAS to ∑PFAS in muscle (top) and liver (bottom). (a) Gournay-Sur-Marne, (b) Levallois, (c) Le Pecq, (d) Triel-Sur-Seine. PFAS were color-coded: pink = PFCAs, green = PFSAs, red = FTSAs, yellow = (N-alkyl)-FASAAs; orange = (N-alkyl)-FASAs, grey = "other PFAS". Note that a logarithmic scale was used for the y-axis.

3.4. Tissue distribution

As expected, PFAS concentrations were higher in liver than in muscle; liver-to-muscle ratios (LMRs) were systematically higher than 1 except for 5:3 FTCA (Table S10). LMRs for PFAAs and FOSA were consistent with previously published values for *Cyprinids* (Labadie and Chevreuil, 2011; Babut et al., 2017; Wu et al., 2019). These are, however, the first data for the emerging PFAS listed in Table S10, which tissue distribution is not documented. Large inter-individual variations LMRs were usually observed: the highest inter-individual variation was for FOSA and 8:2 FTSA (i.e. > 60%), while other PFAS displayed relative standard deviations in the range 33–51%. LMRs computed for 10:2 FTSA, the most recurring FTSA, were similar to those calculated for PFUnDA (5.9±1.9 vs 5.1±1.9), which exhibits a similar perfluoroalkyl chain length, but approximately twice lower than those of L-PFOS (10.7±3.5) likely because of different binding affinity for muscle/liver proteins.

Correlations between PFAS levels in liver and muscle were also explored for analytes with DF > 90%. Significant associations were found for all tested compounds and R^2 ranged from 0.31 to 0.70 (Figure S4). This indicated that hepatic and muscular levels were related although the relation was sometimes weak, in good agreement with the variable LMRs presented above. The lowest correlation coefficient reported for FOSA was possibly due to inter-individual differences in hepatic biotransformation capacities (i.e. conversion of FOSA to PFOS (Letcher et al., 2014)).

3.5. Influence of selected factors on the bioaccumulation of PFAS

To investigate the controlling factors of PFAS bioaccumulation in European Chub, an ANCOVA was performed based on PFAS levels in fish muscle. Such analysis is equivalent to a multiple linear regression including quantitative and qualitative variables (Babut et al., 2017). As demonstrated above, sampling site was a potential determinant of PFAS levels in fish (i.e. contamination gradient/spatial heterogeneity) and a potential confounding factor (i.e. differences in fish C and N isotopic signatures across sites). Thus, it was included as a categorical variable, along with sex (Peng et al., 2010). Explanatory quantitative variables were fish length and trophic ecology proxies (i.e. $\delta^{13}C$ and $\delta^{15}N$). Fish weight was not included as it was strongly correlated with fish length (Figure S5). The latter is often used as a proxy for fish age, thus being more relevant for bioaccumulation studies. PFAS with DF > 90% (*i.e.* C_{10}-C_{14} PFCAs, PFOS, FOSA and 10:2 FTSA) were chosen as response variables. Significant variables and models coefficients are presented in Table 2.

Table 2. ANCOVA results for selected PFAS. Regression coefficients for significant quantitative variables are given in the right-hand column. CI: confidence interval.

	Variables	Adjusted R^2 (p-value)	Variables (p-value)	Coefficients for significant quantitative variables (95% CI)
PFDA	Length, $\delta^{13}C$, $\delta^{15}N$ / Site, Sex	0.46 ($p < 0.0001$)	Length (0.336); $\delta^{15}N$ (0.163); $\delta^{13}C$ (0.006) / Site (<0.0001); Sex (0.529)	
	$\delta^{13}C$ / Site	0.47 ($p < 0.0001$)	$\delta^{13}C$ (0.005) / Site (<0.0001)	$\delta^{13}C$: 0.39 (0.12–0.66)
PFUnDA	Length, $\delta^{13}C$, $\delta^{15}N$ / Site, Sex	0.47 ($p < 0.0001$)	Length (0.290); $\delta^{15}N$ (0.014); $\delta^{13}C$ (<0.001) / Site (<0.0001); Sex (0.869)	
	$\delta^{13}C$, $\delta^{15}N$ / Site	0.49 ($p < 0.0001$)	$\delta^{13}C$ (<0.001); $\delta^{15}N$ (0.016) / Site (<0.0001)	$\delta^{13}C$: 0.49 (0.23–0.76) $\delta^{15}N$: 0.36 (0.07–0.66)
PFDoDA	Length, $\delta^{13}C$, $\delta^{15}N$ / Site, Sex	0.47 ($p < 0.0001$)	Length (0.873); $\delta^{15}N$ (0.002); $\delta^{13}C$ (0.004) / Site (<0.0001); Sex (0.777)	
	$\delta^{13}C$, $\delta^{15}N$ / Site	0.49 ($p < 0.0001$)	$\delta^{13}C$ (0.003); $\delta^{15}N$ (<0.001) / Site (<0.0001)	$\delta^{13}C$: 0.41 (0.15–0.67) $\delta^{15}N$: 0.61 (0.32–0.90)
PFTrDA	Length, $\delta^{13}C$, $\delta^{15}N$ / Site, Sex	0.51 ($p < 0.0001$)	Length (0.550); $\delta^{15}N$ (0.004); $\delta^{13}C$ (0.005) / Site (<0.001); Sex (0.924)	
	$\delta^{13}C$, $\delta^{15}N$ / Site	0.50 ($p < 0.0001$)	$\delta^{13}C$ (0.004); $\delta^{15}N$ (<0.001) / Site (<0.001)	$\delta^{13}C$: 0.39 (0.14–0.65) $\delta^{15}N$: 0.66 (0.37–0.95)
PFTeDA	Length, $\delta^{13}C$, $\delta^{15}N$ / Site, Sex	0.48 ($p < 0.0001$)	Length (0.311); $\delta^{15}N$ (0.004); $\delta^{13}C$ (0.006) / Site (0.005); Sex (0.807)	
	$\delta^{13}C$, $\delta^{15}N$ / Site	0.49 ($p < 0.0001$)	$\delta^{13}C$ (0.006); $\delta^{15}N$ (<0.001) / Site (<0.001)	$\delta^{13}C$: 0.38 (0.12–0.64) $\delta^{15}N$: 0.72 (0.43–1.01)
PFOS	Length, $\delta^{13}C$, $\delta^{15}N$ / Site, Sex	0.51 ($p < 0.0001$)	Length (0.687); $\delta^{15}N$ (0.031); $\delta^{13}C$ (<0.001) / Site (<0.001); Sex (0.274)	
	$\delta^{13}C$, $\delta^{15}N$ / Site	0.51 ($p < 0.0001$)	$\delta^{13}C$ (<0.001); $\delta^{15}N$ (<0.001) / Site (<0.0001)	$\delta^{13}C$: 0.52 (0.27–0.78) $\delta^{15}N$: 0.52 (0.23–0.80)
10:2 FTSA	Length, $\delta^{13}C$, $\delta^{15}N$ / Site, Sex	0.50 ($p < 0.0001$)	Length (0.721); $\delta^{15}N$ (0.566); $\delta^{13}C$ (0.734) / Site (<0.0001); Sex (0.854)	
	Site	0.54 ($p < 0.0001$)	Site (<0.0001)	
FOSA	Length, $\delta^{13}C$, $\delta^{15}N$ / Site, Sex	0.49 ($p < 0.0001$)	Length (0.356); $\delta^{15}N$ (0.432); $\delta^{13}C$ (0.483) / Site (<0.0001); Sex (0.956)	
	Site	0.52 ($p < 0.0001$)	Site (<0.0001)	

For all tested compounds, regression models were significant when all variables were included (Table 2). R^2 ranged between 0.47 and 0.54 (PFDA and 10:2 FTSA, respectively) with *sampling site* being highly significant for all compounds. When the latter was not taken into account, regression models were still significant for PFDoDA, PFTrDA, PFTeDA and PFOS (R^2 = 0.18, 0.23, 0.30 and 0.25, respectively; data not shown in Table 2).

Maternal transfer is a likely elimination pathway in fish (Peng et al., 2010), thereby potentially inducing sex-specific accumulation levels and patterns. Here, however, sex was not a significant variable. This indicates that PFAS bioaccumulation in European chub was not sex-dependent for the life stages considered in our study (i.e. mostly immature individuals), as observed elsewhere (Gewurtz et al., 2012; Pan et al., 2014; Arinaitwe et al., 2020; Schultes et al., 2020). Here, fish length influence was not significant, while it was an important driver of PFAS bioaccumulation in the cyprinid *Barbus barbus* from the Rhône River (Babut et al., 2017) or in the common sole *Solea solea* from the Gironde estuary (Munoz et al., 2017a). In these studies, higher levels were found in smaller individuals because of lower elimination rates and growth dilution. A plausible explanation for this discrepancy might come from the absence of very young juveniles in the present study (i.e. no individuals below 17 cm). As hypothesized, PFAS bioaccumulation in European chub was significantly influenced by diet, to an extent varying according to the compound. However, other factors were likely at a play, as evidenced by the coefficients of determination of the multiple regressions (e.g. contamination gradient, respiratory exposure).

For FOSA and 10:2 FTSA, sampling site was the only significant variable among those tested in the present study. Conversely, PFDA bioaccumulation was also dependent on $\delta^{13}C$ while PFUnDA, PFDoDA, PFTrDA, PFTeDA and PFOS bioaccumulation was significantly controlled by both $\delta^{13}C$ and $\delta^{15}N$. We therefore show that diet is a major controlling factor of PFAS bioaccumulation in an omnivorous river fish species such as European chub. The

influence of $\delta^{15}N$ is consistent with the biomagnification of these PFAS, as observed in various aquatic environments (Simonnet-Laprade et al., 2019; Penland et al., 2020; Pan et al., 2021). Carbon sources in lotic systems are complex (Ishikawa et al., 2012) and more negative $\delta^{13}C$ are mostly linked to detrital organic matter in river, i.e. a carbon source linked with sediments (Finlay, 2001). Since positive coefficients were found for $\delta^{13}C$ (Table 2), PFAS levels tended to increase with $\delta^{13}C$. This strongly suggests that chub that feed more on autochthonous carbon sources (e.g. periphytic biofilm or biofilm grazers) are more exposed to PFAS. Such a result is consistent with PFAS accumulation in biofilms, proven to exceed that observed in sediments (Munoz et al., 2018).

In addition, data transformation allowed ranking model coefficients to determine their relative weight. We found that the 95% confidence intervals of model coefficients overlapped for $\delta^{15}N$ and $\delta^{13}C$. Thus, our findings indicate that both factors exhibited similar weights; carbon sources use is therefore equally important as trophic position to explain within-species variability of PFAS bioaccumulation in *S. cephalus*.

Overall, while other exposure pathways are likely important, e.g. respiratory uptake across the gills (Armitage et al., 2017), uptake via the diet and dietary habits appeared to significantly influence the interindividual variability of PFAS levels in European chub from a river under urban influence. In such rivers, dissolved PFAS concentrations may rapidly vary depending on hydrological conditions (Munoz et al., 2018). The relative influence of each parameters should be further investigated on different chub populations and different species to confirm these results, while other relevant variables such as protein/phospholipid content could also be considered (Armitage et al., 2013).

4. Conclusion

This study investigated an extended list of PFAS in sediment and fish along a longitudinal transect in the Seine River basin. The results suggest that the Greater Paris has a strong influence on PFAS inputs in the Seine River. We demonstrated the widespread occurrence in sediment and fish of PFAS of emerging concern such as FTABs and FTSAs, usually linked to point sources related to firefighting or industrial activities. In particular, 6:2 FTAB was prevalent in most sediments, while 10:2 FTSA was ubiquitous in fish. Such findings highlight the need for suitable quantitative analytical methods to address a wide range of target compounds, which is mandatory to better understand PFAS occurrence and fate in hydrosystems. PFAS levels in fish were dependent on the sampling site, but trophic ecology significantly explained interindividual variations; trophic level and carbon sources displayed similar weights. However, while such drivers are influential, they are not sufficient to fully explain PFAS bioaccumulation in European chub at the individual level. Future research is therefore needed to get further insight into this issue.

Declaration of competing interest

The authors declare that they have no known competing financial interests or personal relationships that could have appeared to influence the work reported in this paper.

Acknowledgments

This study was supported by the PIREN-Seine and MeSeine Innovation programs, along with the Investments for the Future Program (Cluster of Excellence COTE, ANR-10-LABX-45). CPER A2E (Aquitaine region), E3A (Aquitaine region) and FEDER (“Europe is moving in

Aquitaine with the European Regional Development Fund") are also acknowledged for funding. PFAS and stable isotope analyses were performed using the technical facilities from the PLATINE mass spectrometry platform at UMR 5805 EPOC. We are grateful to V. Lespannier (Aquascope) for his support on the sampling campaign and to A. Coynel (UMR 5805 EPOC) who supplied total organic carbon data.

Appendix. Supplementary Information

References

Ahrens, L., 2011. Polyfluoroalkyl compounds in the aquatic environment: a review of their occurrence and fate. J. Environ. Monit. 13, 20–31. https://doi.org/10.1039/C0EM00373E

Ahrens, L., Norström, K., Viktor, T., Cousins, A.P., Josefsson, S., 2015. Stockholm Arlanda Airport as a source of per- and polyfluoroalkyl substances to water, sediment and fish. Chemosphere 129, 33–38. https://doi.org/10.1016/j.chemosphere.2014.03.136

Åkerblom, S., Negm, N., Wu, P., Bishop, K., Ahrens, L., 2017. Variation and accumulation patterns of poly- and perfluoroalkyl substances (PFAS) in European perch (Perca fluviatilis) across a gradient of pristine Swedish lakes. Science of The Total Environment 599–600, 1685–1692. https://doi.org/10.1016/j.scitotenv.2017.05.032

Allred, B.M., Lang, J.R., Barlaz, M.A., Field, J.A., 2015. Physical and Biological Release of Poly- and Perfluoroalkyl Substances (PFASs) from Municipal Solid Waste in Anaerobic Model Landfill Reactors. Environ. Sci. Technol. 49, 7648–7656. https://doi.org/10.1021/acs.est.5b01040

Arinaitwe, K., Koch, A., Taabu-Munyaho, A., Marien, K., Reemtsma, T., Berger, U., 2020. Spatial profiles of perfluoroalkyl substances and mercury in fish from northern Lake Victoria, East Africa. Chemosphere 260, 127536. https://doi.org/10.1016/j.chemosphere.2020.127536

Armitage, J.M., Arnot, J.A., Wania, F., Mackay, D., 2013. Development and evaluation of a mechanistic bioconcentration model for ionogenic organic chemicals in fish. Environmental Toxicology and Chemistry 32, 115–128. https://doi.org/10.1002/etc.2020

Armitage, J.M., Erickson, R.J., Luckenbach, T., Ng, C.A., Prosser, R.S., Arnot, J.A., Schirmer, K., Nichols, J.W., 2017. Assessing the bioaccumulation potential of ionizable organic compounds: Current knowledge and research priorities. Environmental Toxicology and Chemistry 36, 882–897. https://doi.org/10.1002/etc.3680

Azimi, S., Rocher, V., 2016. Influence of the water quality improvement on fish population in the Seine River (Paris, France) over the 1990–2013 period. Science of The Total Environment 542, 955–964. https://doi.org/10.1016/j.scitotenv.2015.10.094

Babut, M., Labadie, P., Simonnet-Laprade, C., Munoz, G., Roger, M.-C., Ferrari, B.J.D., Budzinski, H., Sivade, E., 2017. Per- and poly-fluoroalkyl compounds in freshwater fish from the Rhône River: Influence of fish size, diet, prey contamination and biotransformation. Science of The Total Environment 605–606, 38–47. https://doi.org/10.1016/j.scitotenv.2017.06.111

Balestrieri, A., Prigioni, C., Remonti, L., Sgrosso, S., Priore, G., 2006. Feeding ecology of Leuciscus cephalus and Rutilus rubilio in southern Italy. Italian Journal of Zoology 73, 129–135. https://doi.org/10.1080/11250000600679561

Banque Hydro, http://www.hydro.eaufrance.fr/ (accessed 30/10/2021)Barzen-Hanson, K.A., Davis, S.E., Kleber, M., Field, J.A., 2017. Sorption of Fluorotelomer Sulfonates, Fluorotelomer Sulfonamido Betaines, and a Fluorotelomer Sulfonamido Amine in National Foam Aqueous Film-Forming Foam to Soil. Environmental Science & Technology 51, 12394–12404. https://doi.org/10.1021/acs.est.7b03452

Bodin, N., Budzinski, H., Le Ménach, K., Tapie, N., 2009. ASE extraction method for simultaneous carbon and nitrogen stable isotope analysis in soft tissues of aquatic organisms. Analytica Chimica Acta 643, 54–60. https://doi.org/10.1016/j.aca.2009.03.048

Boiteux, V., Dauchy, X., Bach, C., Colin, A., Hemard, J., Sagres, V., Rosin, C., Munoz, J.-F., 2017. Concentrations and patterns of perfluoroalkyl and polyfluoroalkyl substances in a river and three drinking water treatment plants near and far from a major production source. Science of The Total Environment 583, 393–400. https://doi.org/10.1016/j.scitotenv.2017.01.079

Butt, C.M., Muir, D.C.G., Mabury, S.A., 2014. Biotransformation pathways of fluorotelomer-based polyfluoroalkyl substances: A review. Environmental Toxicology and Chemistry 33, 243–267. https://doi.org/10.1002/etc.2407

Caffrey, J.M., Acevedo, S., Gallagher, K., Britton, R., 2008. Chub (Leuciscus cephalus): a new potentially invasive fish species in Ireland. Aquatic Invasions 3, 201–209.

Cerveny, D., Grabic, R., Fedorova, G., Grabicova, K., Turek, J., Kodes, V., Golovko, O., Zlabek, V., Randak, T. 2016. Perfluoroalkyl Substances in Aquatic Environment-Comparison of Fish and Passive Sampling Approaches. Environ. Res. 144, 92–98. https://doi.org/10.1016/j.envres.2015.11.010.

Chen, H., Munoz, G., Duy, S.V., Zhang, L., Yao, Y., Zhao, Z., Yi, L., Liu, M., Sun, H., Liu, J., Sauvé, S., 2020. Occurrence and Distribution of Per- and Polyfluoroalkyl Substances in Tianjin, China: The Contribution of Emerging and Unknown Analogues. Environ. Sci. Technol. 54, 14254–14264. https://doi.org/10.1021/acs.est.0c00934

Chen, M., Guo, T., He, K., Zhu, L., Jin, H., Wang, Q., Liu, M., Yang, L., 2019. Biotransformation and bioconcentration of 6:2 and 8:2 polyfluoroalkyl phosphate diesters in common carp (Cyprinus carpio): Underestimated ecological risks. Science of The Total Environment 656, 201–208. https://doi.org/10.1016/j.scitotenv.2018.11.297

De Silva, A.O., Spencer, C., Scott, B.F., Backus, S., Muir, D.C.G., 2011. Detection of a Cyclic Perfluorinated Acid, Perfluoroethylcyclohexane Sulfonate, in the Great Lakes of North America. Environ. Sci. Technol. 45, 8060–8066. https://doi.org/10.1021/es200135c

De Silva, A.O.D., Armitage, J.M., Bruton, T.A., Dassuncao, C., Heiger-Bernays, W., Hu, X.C., Kärrman, A., Kelly, B., Ng, C., Robuck, A., Sun, M., Webster, T.F., Sunderland, E.M., 2021. PFAS Exposure Pathways for Humans and Wildlife: A Synthesis of Current Knowledge and Key Gaps in Understanding. Environmental Toxicology and Chemistry 40, 631–657. https://doi.org/10.1002/etc.4935

Elbaz-Poulichet, F., Seidel, J.-L., Casiot, C., Tusseau-Vuillemin, M.-H., 2006. Short-term variability of dissolved trace element concentrations in the Marne and Seine Rivers near Paris. Science of The Total Environment 367, 278–287. https://doi.org/10.1016/j.scitotenv.2005.11.009

European Commission, 2013. Directive 2013/39/EU of the European Parliament and of the Council of 12 August 2013 amending Directives 2000/60/EC and 2008/105/EC as regards priority substances in the field of water policyText with EEA relevance 17.

Field, J.A., Seow, J., 2017. Properties, occurrence, and fate of fluorotelomer sulfonates. Critical Reviews in Environmental Science and Technology 47, 643–691. https://doi.org/10.1080/10643389.2017.1326276

Finlay, J.C., 2001. Stable-Carbon-Isotope Ratios of River Biota:implications for Energy Flow in Lotic Food Webs. Ecology 82, 1052–1064. https://doi.org/10.1890/0012-9658(2001)082[1052:SCIROR]2.0.CO;2

Fliedner, A., Rüdel, H., Lohmann, N., Buchmeier, G., Koschorreck, J., 2018. Biota monitoring under the Water Framework Directive: On tissue choice and fish species selection. Environmental Pollution 235, 129–140. https://doi.org/10.1016/j.envpol.2017.12.052

Gebbink, W.A., Bossi, R., Rigét, F.F., Rosing-Asvid, A., Sonne, C., Dietz, R., 2016. Observation of emerging per- and polyfluoroalkyl substances (PFASs) in Greenland marine mammals. Chemosphere 144, 2384–2391. https://doi.org/10.1016/j.chemosphere.2015.10.116

Gewurtz, S.B., De Silva, A.O., Backus, S.M., McGoldrick, D.J., Keir, M.J., Small, J., Melymuk, L., Muir, D.C.G., 2012. Perfluoroalkyl Contaminants in Lake Ontario Lake Trout: Detailed Examination of Current Status and Long-Term Trends. Environ. Sci. Technol. 46, 5842–5850. https://doi.org/10.1021/es3006095

Giesy, J.P., Kannan, K., 2001. Global Distribution of Perfluorooctane Sulfonate in Wildlife. Environmental Science & Technology 35, 1339–1342. https://doi.org/10.1021/es001834k

Grosbois, C., Meybeck, M., Horowitz, A., Ficht, A., 2006. The spatial and temporal trends of Cd, Cu, Hg, Pb and Zn in Seine River floodplain deposits (1994–2000). Science of The Total Environment 356, 22–37. https://doi.org/10.1016/j.scitotenv.2005.01.049

Hamid, H., Li, L.Y., Grace, J.R., 2020. Aerobic biotransformation of fluorotelomer compounds in landfill leachate-sediment. Science of The Total Environment 713, 136547. https://doi.org/10.1016/j.scitotenv.2020.136547

Hansen, K.J., Clemen, L.A., Ellefson, M.E., Johnson, H.O., 2001. Compound-Specific, Quantitative Characterization of Organic Fluorochemicals in Biological Matrices. Environmental Science & Technology 35, 766–770. https://doi.org/10.1021/es001489z

Hette Tronquart, N., Belliard, J., Tales, E., Oberdorff, T., 2016. Stable isotopes reveal food web modifications along the upstream-downstream gradient of a temperate stream. Aquatic Sciences - Research Across Boundaries 78, 255–265. https://doi.org/10.1007/s00027-015-0421-8

Hicks, K.A., Loomer, H.A., Fuzzen, M.L.M., Kleywegt, S., Tetreault, G.R., McMaster, M.E., Servos, M.R., 2017. δ15N tracks changes in the assimilation of sewage-derived nutrients into a riverine food web before and after major process alterations at two municipal wastewater treatment plants. Ecological Indicators 72, 747–758. https://doi.org/10.1016/j.ecolind.2016.09.011

Ishikawa, N.F., Doi, H., Finlay, J.C., 2012. Global meta-analysis for controlling factors on carbon stable isotope ratios of lotic periphyton. Oecologia 170, 541–549. https://doi.org/10.1007/s00442-012-2308-x

Jin, B., Mallula, S., Golovko, S.A., Golovko, M.Y., Xiao, F., 2020. In Vivo Generation of PFOA, PFOS, and Other Compounds from Cationic and Zwitterionic Per- and Polyfluoroalkyl Substances in a Terrestrial Invertebrate (*Lumbricus terrestris*). Environ. Sci. Technol. 54, 7378–7387. https://doi.org/10.1021/acs.est.0c01644

Joerss, H., Apel, C., Ebinghaus, R., 2019. Emerging per- and polyfluoroalkyl substances (PFASs) in surface water and sediment of the North and Baltic Seas. Science of The Total Environment 686, 360–369. https://doi.org/10.1016/j.scitotenv.2019.05.363

Labadie, P., Chevreuil, M., 2011. Partitioning behaviour of perfluorinated alkyl contaminants between water, sediment and fish in the Orge River (nearby Paris, France). Environmental Pollution 159, 391–397. https://doi.org/10.1016/j.envpol.2010.10.039

Langberg, H.A., Breedveld, G.D., Grønning, H.M., Kvennås, M., Jenssen, B.M., Hale, S.E., 2019. Bioaccumulation of Fluorotelomer Sulfonates and Perfluoroalkyl Acids in Marine Organisms Living in Aqueous Film-Forming Foam Impacted Waters. Environ. Sci. Technol. acs.est.9b00927. https://doi.org/10.1021/acs.est.9b00927

Lee, Y.-M., Lee, J.-Y., Kim, M.-K., Yang, H., Lee, J.-E., Son, Y., Kho, Y., Choi, K., Zoh, K.-D., 2020. Concentration and distribution of per- and polyfluoroalkyl substances

(PFAS) in the Asan Lake area of South Korea. Journal of Hazardous Materials 381, 120909. https://doi.org/10.1016/j.jhazmat.2019.120909

Lescord, G.L., Kidd, K.A., De Silva, A.O., Williamson, M., Spencer, C., Wang, X., Muir, D.C.G., 2015. Perfluorinated and Polyfluorinated Compounds in Lake Food Webs from the Canadian High Arctic. Environ. Sci. Technol. 49, 2694–2702. https://doi.org/10.1021/es5048649

Letcher, R.J., Chu, S., McKinney, M.A., Tomy, G.T., Sonne, C., Dietz, R., 2014. Comparative hepatic in vitro depletion and metabolite formation of major perfluorooctane sulfonate precursors in arctic polar bear, beluga whale, and ringed seal. Chemosphere 112, 225–231. https://doi.org/10.1016/j.chemosphere.2014.04.022

Liu, J., Wang, N., Szostek, B., Buck, R.C., Panciroli, P.K., Folsom, P.W., Sulecki, L.M., Bellin, C.A., 2010. 6-2 Fluorotelomer alcohol aerobic biodegradation in soil and mixed bacterial culture. Chemosphere 78, 437–444. https://doi.org/10.1016/j.chemosphere.2009.10.044

Liu, Y., Ruan, T., Lin, Y., Liu, A., Yu, M., Liu, R., Meng, M., Wang, Y., Liu, J., Jiang, G., 2017. Chlorinated Polyfluoroalkyl Ether Sulfonic Acids in Marine Organisms from Bohai Sea, China: Occurrence, Temporal Variations, and Trophic Transfer Behavior. Environ. Sci. Technol. 51, 4407–4414. https://doi.org/10.1021/acs.est.6b06593

Loi, E.I.H., Yeung, L.W.Y., Taniyasu, S., Lam, P.K.S., Kannan, K., Yamashita, N., 2011. Trophic Magnification of Poly- and Perfluorinated Compounds in a Subtropical Food Web. Environmental Science & Technology 45, 5506–5513. https://doi.org/10.1021/es200432n

Lopes, C., Perga, M.-E., Peretti, A., Roger, M.-C., Persat, H., Babut, M., 2011. Is PCBs concentration variability between and within freshwater fish species explained by their contamination pathways? Chemosphere 85, 502–508. https://doi.org/10.1016/j.chemosphere.2011.08.011

Mann, R.H.K., 1976. Observations on the age, growth, reproduction and food of the chub Squalius cephalus (L.) in the River Stour, Dorset. Journal of Fish Biology 8, 265–288. https://doi.org/10.1111/j.1095-8649.1976.tb03950.x

Marković, G.S., Simić, V.M., Ostojić, A.M., Simić, S.B., 2007. Seasonal variation in nutrition of chub (Leuciscus cephalus L., Cyprinidae, Osteichthyes) in one reservoir of West Serbia. Zbornik Matice srpske za prirodne nauke 107–113.

Munoz, G., Budzinski, H., Babut, M., Drouineau, H., Lauzent, M., Menach, K.L., Lobry, J., Selleslagh, J., Simonnet-Laprade, C., Labadie, P., 2017a. Evidence for the Trophic Transfer of Perfluoroalkylated Substances in a Temperate Macrotidal Estuary. Environ. Sci. Technol. 51, 8450–8459. https://doi.org/10.1021/acs.est.7b02399

Munoz, G., Desrosiers, M., Duy, S.V., Labadie, P., Budzinski, H., Liu, J., Sauvé, S., 2017b. Environmental Occurrence of Perfluoroalkyl Acids and Novel Fluorotelomer Surfactants in the Freshwater Fish *Catostomus commersonii* and Sediments Following Firefighting Foam Deployment at the Lac-Mégantic Railway Accident. Environ. Sci. Technol. 51, 1231–1240. https://doi.org/10.1021/acs.est.6b05432

Munoz, G., Desrosiers, M., Vetter, L., Vo Duy, S., Jarjour, J., Liu, J., Sauvé, S., 2020. Bioaccumulation of Zwitterionic Polyfluoroalkyl Substances in Earthworms Exposed to Aqueous Film-Forming Foam Impacted Soils. Environ. Sci. Technol. 54, 1687–1697. https://doi.org/10.1021/acs.est.9b05102

Munoz, G., Duy, S.V., Labadie, P., Botta, F., Budzinski, H., Lestremau, F., Liu, J., Sauvé, S., 2016. Analysis of zwitterionic, cationic, and anionic poly- and perfluoroalkyl surfactants in sediments by liquid chromatography polarity-switching electrospray ionization coupled to high resolution mass spectrometry. Talanta 152, 447–456. https://doi.org/10.1016/j.talanta.2016.02.021

Munoz, G., Fechner, L.C., Geneste, E., Pardon, P., Budzinski, H., Labadie, P., 2018. Spatio-temporal dynamics of per and polyfluoroalkyl substances (PFASs) and transfer to periphytic biofilm in an urban river: case-study on the River Seine. Environ Sci Pollut Res 25, 23574–23582. https://doi.org/10.1007/s11356-016-8051-9

Munoz, G., Giraudel, J.-L., Botta, F., Lestremau, F., Dévier, M.-H., Budzinski, H., Labadie, P., 2015. Spatial distribution and partitioning behavior of selected poly- and perfluoroalkyl substances in freshwater ecosystems: A French nationwide survey. Science of The Total Environment 517, 48–56. https://doi.org/10.1016/j.scitotenv.2015.02.043

Munoz, G., Liu, J., Vo Duy, S., Sauvé, S., 2019. Analysis of F-53B, Gen-X, ADONA, and emerging fluoroalkylether substances in environmental and biomonitoring samples: A review. Trends in Environmental Analytical Chemistry e00066. https://doi.org/10.1016/j.teac.2019.e00066

Nyeste, K., Dobrocsi, P., Czeglédi, I., Czédli, H., Harangi, S., Baranyai, E., Simon, E., Nagy, S.A., Antal, L., 2019. Age and diet-specific trace element accumulation patterns in different tissues of chub (Squalius cephalus): Juveniles are useful bioindicators of recent pollution. Ecological Indicators 101, 1–10. https://doi.org/10.1016/j.ecolind.2019.01.001

Pan, C.-G., Xiao, S.-K., Yu, K.-F., Wu, Q., Wang, Y.-H., 2021. Legacy and alternative per- and polyfluoroalkyl substances in a subtropical marine food web from the Beibu Gulf, South China: Fate, trophic transfer and health risk assessment. Journal of Hazardous Materials 403, 123618. https://doi.org/10.1016/j.jhazmat.2020.123618

Pan, C.-G., Zhao, J.-L., Liu, Y.-S., Zhang, Q.-Q., Chen, Z.-F., Lai, H.-J., Peng, F.-J., Liu, S.-S., Ying, G.-G., 2014. Bioaccumulation and risk assessment of per- and polyfluoroalkyl substances in wild freshwater fish from rivers in the Pearl River Delta region, South China. Ecotoxicology and Environmental Safety 107, 192–199. https://doi.org/10.1016/j.ecoenv.2014.05.031

Pan, Y., Zhang, H., Cui, Q., Sheng, N., Yeung, L.W.Y., Sun, Y., Guo, Y., Dai, J., 2018. Worldwide Distribution of Novel Perfluoroether Carboxylic and Sulfonic Acids in Surface Water. Environ. Sci. Technol. 52, 7621–7629. https://doi.org/10.1021/acs.est.8b00829

Peng, H., Wei, Q., Wan, Y., Giesy, J.P., Li, L., Hu, J., 2010. Tissue Distribution and Maternal Transfer of Poly- and Perfluorinated Compounds in Chinese Sturgeon (Acipenser sinensis): Implications for Reproductive Risk. Environ. Sci. Technol. 44, 1868–1874. https://doi.org/10.1021/es903248d

Penland, T.N., Cope, W.G., Kwak, T.J., Strynar, M.J., Grieshaber, C.A., Heise, R.J., Sessions, F.W., 2020. Trophodynamics of Per- and Polyfluoroalkyl Substances in the Food Web of a Large Atlantic Slope River. Environ. Sci. Technol. 54, 6800–6811. https://doi.org/10.1021/acs.est.9b05007

Place, B.J., Field, J.A., 2012. Identification of Novel Fluorochemicals in Aqueous Film-Forming Foams Used by the US Military. Environ. Sci. Technol. 46, 7120–7127. https://doi.org/10.1021/es301465n

Schultes, L., Sandblom, O., Broeg, K., Bignert, A., Benskin, J.P., 2020. Temporal Trends (1981–2013) of Per- and Polyfluoroalkyl Substances and Total Fluorine in Baltic cod (Gadus morhua). Environmental Toxicology and Chemistry 39, 300–309. https://doi.org/10.1002/etc.4615

Shi, G., Cui, Q., Zhang, H., Cui, R., Guo, Y., Dai, J., 2019. Accumulation, Biotransformation, and Endocrine Disruption Effects of Fluorotelomer Surfactant Mixtures on Zebrafish. Chem. Res. Toxicol. 32, 1432–1440. https://doi.org/10.1021/acs.chemrestox.9b00127

Shi, Y., Vestergren, R., Zhou, Z., Song, X., Xu, L., Liang, Y., Cai, Y., 2015. Tissue Distribution and Whole Body Burden of the Chlorinated Polyfluoroalkyl Ether Sulfonic Acid F-53B in Crucian Carp (Carassius carassius): Evidence for a Highly Bioaccumulative Contaminant of Emerging Concern. Environ. Sci. Technol. 49, 14156–14165. https://doi.org/10.1021/acs.est.5b04299

Simonnet-Laprade, C., Budzinski, H., Maciejewski, K., Le Menach, K., Santos, R., Alliot, F., Goutte, A., Labadie, P., 2019. Biomagnification of perfluoroalkyl acids (PFAAs) in the food web of an urban river: assessment of the trophic transfer of targeted and unknown precursors and implications. Environ. Sci.: Processes Impacts 10.1039.C9EM00322C. https://doi.org/10.1039/C9EM00322C

Teil, M.-J., Tlili, K., Blanchard, M., Labadie, P., Alliot, F., Chevreuil, M., 2014. Polychlorinated Biphenyls, Polybrominated Diphenyl Ethers, and Phthalates in Roach from the Seine River Basin (France): Impact of Densely Urbanized Areas. Arch Environ Contam Toxicol 66, 41–57. https://doi.org/10.1007/s00244-013-9955-8

Tu, W., Martínez, R., Navarro-Martin, L., Kostyniuk, D.J., Hum, C., Huang, J., Deng, M., Jin, Y., Chan, H.M., Mennigen, J.A., 2019. Bioconcentration and Metabolic Effects of Emerging PFOS Alternatives in Developing Zebrafish. Environ. Sci. Technol. acs.est.9b03820. https://doi.org/10.1021/acs.est.9b03820

Wang, Q., Ruan, Y., Jin, L., Zhang, X., Li, J., He, Y., Wei, S., Lam, J.C.W., Lam, P.K.S., 2021. Target, Nontarget, and Suspect Screening and Temporal Trends of Per- and Polyfluoroalkyl Substances in Marine Mammals from the South China Sea. Environ. Sci. Technol. 55, 1045–1056. https://doi.org/10.1021/acs.est.0c06685

Wang, S., Huang, J., Yang, Y., Hui, Y., Ge, Y., Larssen, T., Yu, G., Deng, S., Wang, B., Harman, C., 2013. First Report of a Chinese PFOS Alternative Overlooked for 30 Years: Its Toxicity, Persistence, and Presence in the Environment. Environmental Science & Technology 47, 10163–10170. https://doi.org/10.1021/es401525n

Wang, Y., Vestergren, R., Shi, Y., Cao, D., Xu, L., Cai, Y., Zhao, X., Wu, F., 2016. Identification, Tissue Distribution, and Bioaccumulation Potential of Cyclic Perfluorinated Sulfonic Acids Isomers in an Airport Impacted Ecosystem. Environ. Sci. Technol. 50, 10923–10932. https://doi.org/10.1021/acs.est.6b01980

Wen, W., Xia, X., Hu, D., Zhou, D., Wang, H., Zhai, Y., Lin, H., 2017. Long-Chain Perfluoroalkyl acids (PFAAs) Affect the Bioconcentration and Tissue Distribution of Short-Chain PFAAs in Zebrafish (Danio rerio). Environ. Sci. Technol. 51, 12358–12368. https://doi.org/10.1021/acs.est.7b03647

Wu, J.-Y., Liu, W.-X., He, W., Xu, F.-L., 2019. Comparisons of tissue distributions and health risks of perfluoroalkyl acids (PFAAs) in two fish species with different trophic levels from Lake Chaohu, China. Ecotoxicology and Environmental Safety 185, 109666. https://doi.org/10.1016/j.ecoenv.2019.109666

Xiao, F., 2017. Emerging poly- and perfluoroalkyl substances in the aquatic environment: A review of current literature. Water Research 124, 482–495. https://doi.org/10.1016/j.watres.2017.07.024

Zabaleta, I., Bizkarguenaga, E., Izagirre, U., Negreira, N., Covaci, A., Benskin, J.P., Prieto, A., Zuloaga, O., 2017. Biotransformation of 8:2 polyfluoroalkyl phosphate diester in gilthead bream (Sparus aurata). Science of The Total Environment 609, 1085–1092. https://doi.org/10.1016/j.scitotenv.2017.07.241

Zhang, W., Pang, S., Lin, Z., Mishra, S., Bhatt, P., Chen, S., 2021. Biotransformation of perfluoroalkyl acid precursors from various environmental systems: advances and perspectives. Environmental Pollution 272, 115908. https://doi.org/10.1016/j.envpol.2020.115908